Bainite in silicon steels: new composition–property approach Part 2

H. K. D. H. Bhadeshia and D. V. Edmonds

Research discussed in Part 1 of this study indicated that the properties of microstructures based on bainitic ferrite and carbon enriched retained austenite can be optimized by ensuring that the austenite exhibits both mechanical and thermal stability. These conditions were quantitatively described in terms of a criterion comprising the volume fraction of bainitic ferrite and other terms deduced experimentally. This paper reports the testing and further development of this criterion: the volume fraction of bainitic ferrite (and hence the carbon content of the residual austenite) can be thermodynamically estimated from a knowledge of the steel composition and the isothermal transformation temperature only. Using thermodynamics, it was predicted that two steel compositions in particular should yield even better properties than have been obtained previously. Therefore, these steels were prepared and tested, and the impact properties at very high strength levels were shown to be much improved. MS/0811b

 Manuscript received 23 March 1982; in final form 10 December 1982. H. K. D. H. Bhadeshia is in the Department of Metallurgy and Materials Science, University of Cambridge and D. V. Edmonds is in the Department of Metallurgy and Science of Materials, University of Oxford.

The principal steel (Fe–0·43C–3·0Mn–2·02Si, wt-%) which was the subject of Part 1 of this study[1] was found to exhibit optimum strength and toughness in the bainitic condition. Nevertheless, the *absolute* toughness levels encountered even with the bainitic microstructures were inadequate since the impact transition temperatures observed were well above ambient.

The results also indicated[1] that the blocky morphology of retained austenite is detrimental to toughness and is unstable relative to the film morphology of retained austenite. It is this instability (both to martensitic transformation during the quench from the isothermal transformation temperature and to stress induced martensitic transformation) that appears to lead to poor toughness, and the stage at which blocky austenite does not *determine* the overall toughness was described in Part 1 in terms of the following criterion

$$(V_{\gamma-f}/V_{\gamma-B}) = V_b/(6-7{\cdot}7V_b) > 0{\cdot}9 \quad . \quad . \quad . \quad . \quad . \quad . \quad (1)$$

The first three terms represent the volume fractions of film type retained austenite, blocky retained austenite, and bainitic ferrite, respectively. Equation (1) indicates that the best properties would be expected when the ratio $(V_{\gamma-f}/V_{\gamma-B})$ is a maximum. Maximization of this ratio is equivalent to increasing the degree of isothermal transformation permitted (by the thermodynamic condition that the free energy change for diffusionless transformation be negative) at any given temperature within the bainitic transformation range. This would not only promote the further (post-transformation) partitioning of carbon into the residual austenite, but would also refine and reduce the quantity of blocky austenite. Both these factors should contribute to the required stability. Previous work[2,3] suggested two main methods of increasing the maximum permitted degree of transformation to bainitic ferrite:

(i) by reducing the overall carbon content of the alloy concerned, so that the critical concentration in the austenite at which displacive transformation becomes impossible is reached at a later stage (and hence a higher V_b) in the transformation (*see* equation (1), Part 1). Of course, this is only useful if the reduction of the overall carbon content of the alloy does not at the same time lead to a drop in the strength of the microstructure

(ii) by modifying the substitutional alloying elements such that the T_0 (Refs. 1–3) curves are shifted to higher austenite carbon contents.

The present paper is concerned with the evaluation of both these possibilities.

EXPERIMENTAL METHODS

The experimental methods are essentially the same as in Part 1, and are not restated here. The steels were prepared as 20 kg vacuum induction melts from high purity base materials with final compositions (wt-%) as follows: Fe–0·22C–3·00Mn–2·03Si and Fe–0·39C–4·08Ni–2·05Si. The choice of these particular steels is based on the two maximization concepts of V_b discussed above.

RESULTS AND DISCUSSION

T_0 calculations

The T_0 curves for the Fe–3·00Mn–2·03Si and Fe–4·08Ni–2·05Si alloys are plotted in Fig. 1 as a function of carbon content (*see* Refs. 2 and 3 for details). It should be noted that such curves vary only as a function of the substitutional alloying element content and are unaffected

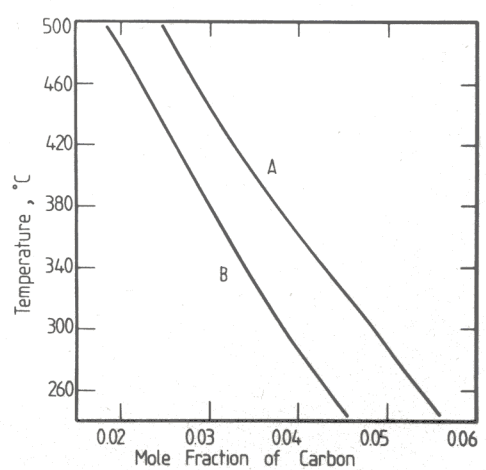

A: Fe–4·08Ni–2·05Si; B: Fe–3·00Mn–2·02Si

1 T_0 curves for steels used in this investigation

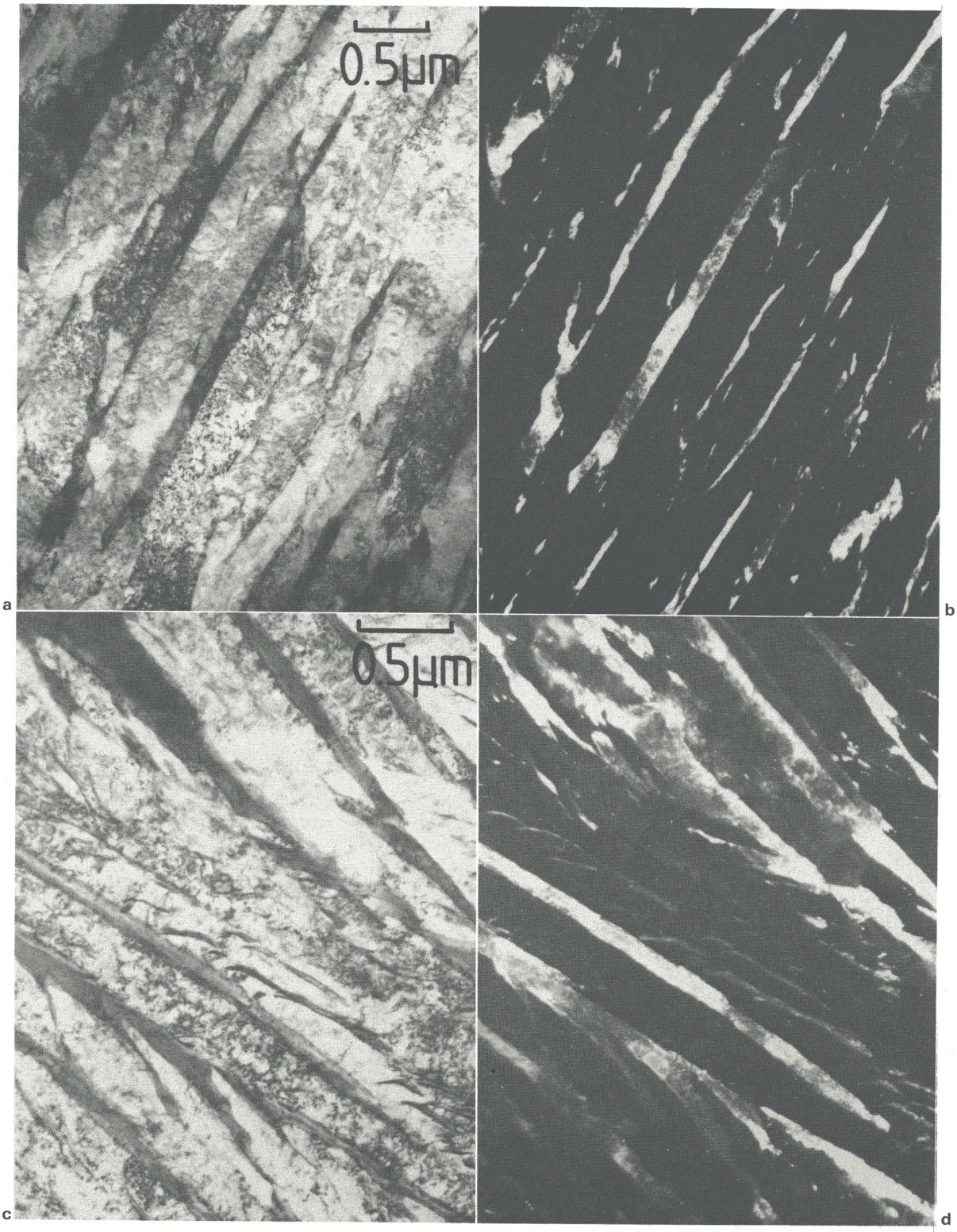

a, b Fe–0·22C–3·00Mn–2·03Si; *c, d* Fe–0·39C–4·08Ni–2·05Si

2 Typical *a, c* bright field and *b, d* retained austenite dark field images of microstructures obtained by isothermal transformation at 340°C

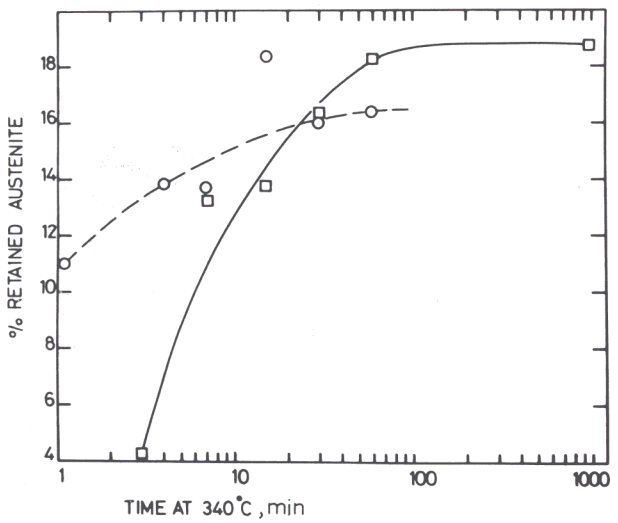

3 Plot of % retained austenite as function of time at isothermal transformation temperature of 340°C

by the average carbon content of the alloy $\bar{x}$. Clearly, for a given value of $\bar{x}$, the austenite in the nickel containing steel can tolerate more carbon before bainitic transformation becomes impossible, thus increasing the maximum permitted value of V_b at any isothermal transformation temperature. Of course, an increase in V_b can also be achieved by reducing $\bar{x}$: for this reason the Fe–0·22C–3·0Mn–2·03Si alloy has about half the carbon content of the Fe–0·43C–3·0Mn–2·02Si alloy studied in Part 1. Hence, both the alloys used should be capable of transforming to higher maximum values of V_b, so that much improved properties can be expected. Furthermore, the strength levels should be maintained at least, despite the alloy modifications, since the volume fraction of bainitic ferrite is expected to increase relative to the amount of residual austenite.

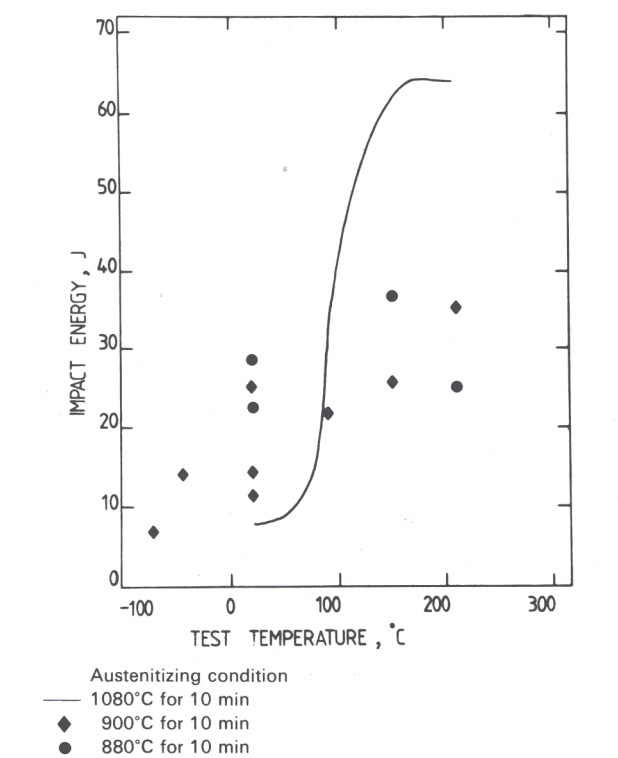

4 Results of impact tests (points) on Fe–0·43C–3·0Mn–2·02Si alloy (Part 1), following isothermal transformation at 295°C for 115 min: curve reproduced from Part 1

Characterization of microstructure

Figure 2 illustrates the microstructures obtained following isothermal transformation at 340°C: detailed examination revealed that both the steels gave microstructures consisting of an aggregate of only bainitic ferrite and retained austenite, as studied in Part 1.

X-ray analysis was used to determine the time periods necessary for the effective termination of transformation at 340°C, and to estimate the quantities of retained austenite involved. Specimens of each alloy were isothermally transformed at 340°C for various time periods before finally water quenching. The results are presented in Fig. 3 which shows that the Fe–0·22C–3·00Mn–2·03Si and Fe–0·39C–2·05Si–4·08Ni alloys require 30 and 60 min respectively in order to achieve reaction termination at 340°C (subsequent isothermal transformations were therefore carried out for these time periods).

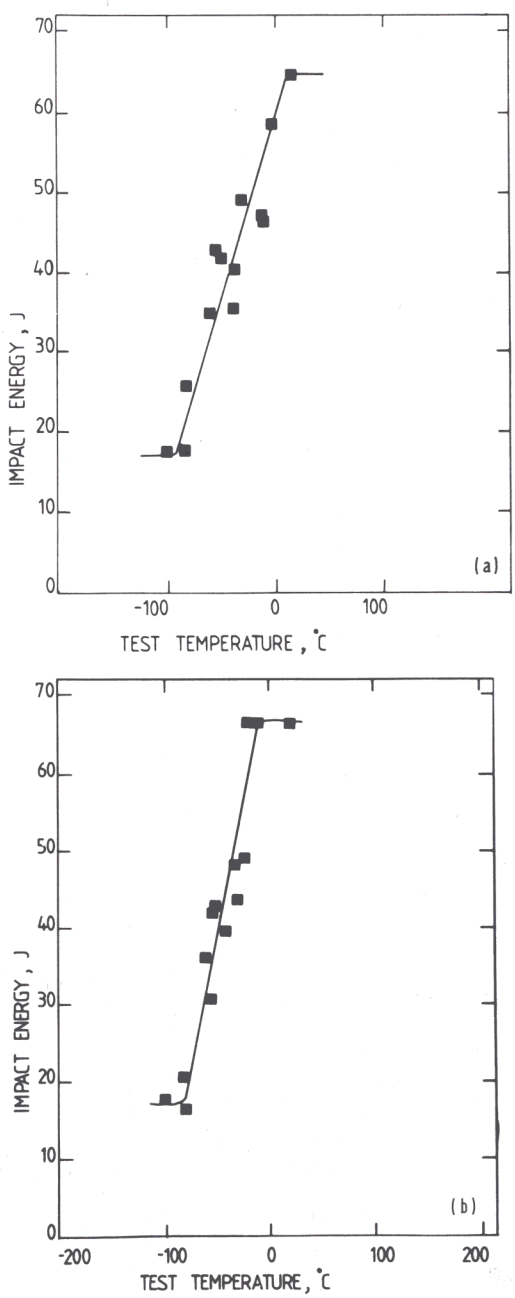

a specimens austenitized at 1080°C for 10 min; *b* specimens austenitized at 880°C for 10 min

5 Impact test results using Fe–0·22C–3·00Mn–2·03Si alloy after isothermal transformation at 340°C for 30 min

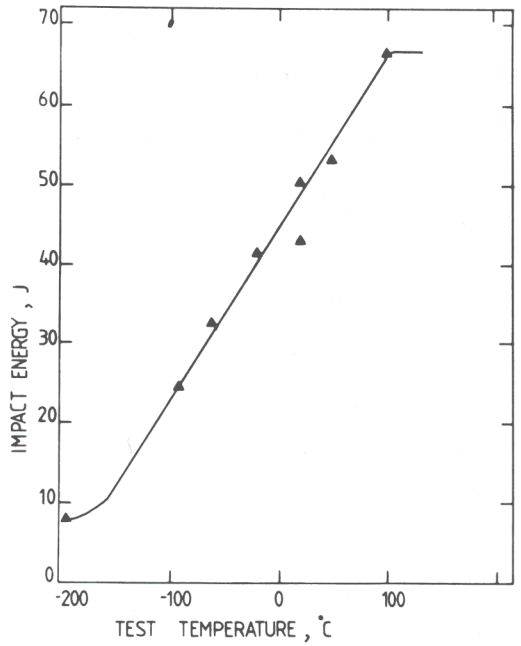

6 Impact transition curve for Fe–0·39C–4·08Ni–2·05Si alloy: 880°C for 10 min, isothermally transformed at 340°C for 60 min, oil quench (OQ)

Impact properties

Varying the austenitizing temperature from 1080 to 880°C did not appear to make any significant difference to the impact properties (Fig. 4), and the latter temperature was used for the remaining part of the study. However, since the purpose of the experiment was to compare the properties of the two alloys with those of the Fe–0·43C–3·0Mn–2·02Si alloy discussed in Part 1, some further tests were performed which confirmed (*see* Fig. 5) that any improvement in properties obtained with the new steels cannot be attributed to the differences in austenitizing conditions.

A comparison of the impact properties presented in Figs. 4 and 6 with the best impact transition curve obtained earlier (Fig. 6*a*, Part 1), clearly indicates that a considerable improvement in toughness has been achieved. Furthermore, this improvement occurs *despite* the fact that the strength of the microstructures involved remains unchanged: the hardness of each specimen studied was about 450 HV. Some calculated and experimental data of the microstructures involved are presented in Table 1. From these data, it is evident that the variation in the carbon content of the retained austenite x_γ does not explain the improved toughness observed with the new alloys. However, the results are consistent with the enhancement of toughness expected when the amount of blocky austenite and martensite are reduced and, in general, when the ratio $V_{\gamma-f}/V_{\gamma-B}$ is increased. (V_γ and $V_{\alpha'}$ are the volume fractions of retained austenite and martensite, respectively.)

Some standard Charpy impact tests were also carried out, in order to provide a basis for comparison with industrially used steels (Table 2). The results obtained are well above the usual impact energies specified for the very high proof stress values indicated.

Tensile tests

The tensile specimens used in the tests were of the standard Hounsfield no. 11 design, with a 3 mm dia. but a 50 mm gauge length. These were heat treated after being machined in the same way as the impact specimens discussed earlier. The results are presented in Table 3. It is probable that the higher strength of the nickel based alloy is largely due to the presence of some martensite and blocky austenite (*see* Table 1) in the microstructure. It is clear that the steels represent a combination of high strength and good ductility.

X-ray analysis of fracture surfaces

The purpose of these experiments was to detect any austenite remaining untransformed at the exposed fracture surfaces of impact specimens. It was hoped to obtain some indication of the stability of retained austenite in the vicinity of the crack tip. X-ray diffraction experiments were conducted with the beam directed at the unmodified fracture surfaces, and calculations[4] indicated that about 50% of the diffracted intensity corresponding to the {111} peak originates from a layer only 3 μm deep, while 95% can be attributed to material from a depth of about 14 μm. These depths are sufficiently small to have been influenced significantly by the events at the crack tip.

Considering that the signal/noise ratio of diffracted information from the fracture surfaces was found to be high, presumably because of intense localized deformation induced during fracture, it was decided to detect the {111} peak since this has the highest structure factor and, hence, is

Table 1 Quantitative data on microstructure and hardness

Alloy, wt-%	Isothermal transformation temperature, °C	V_b	V_γ	$V_{\gamma-f}$	$V_{\gamma-B}$	$V_{\alpha'}$	x_γ, wt-%	Hardness, HV
Fe–0·43C–3·00Mn–2·02Si	295	0·68*	0·22*	0·11	0·11	0·10	0·92	447
Fe–0·43C–3·00Mn–2·02Si	360	0·42*	0·27*	0·06	0·21	0·31	0·79	430
Fe–0·22C–3·00Mn–2·03Si	340	0·84	0·16*	0·16	. .	. .	0·82	430
Fe–0·39C–4·08Ni–2·05Si	340	0·74	0·18*	0·11	0·07	0·08	1·02	450

* Experimental results; the rest of the data being calculated.

Table 2 Charpy impact test and tensile test results

Heat treatment	0·2% proof stress, MN m^{-2}	Impact energy, J	Test temperature, °C
Isothermally transformed at 260°C for 60 min, OQ*	1475	20	−40
	1475	13	−40
	1475	18	25
	1475	20	25
Isothermally transformed at 340°C for 60 min, OQ	1350	29	25
	1350	41	25
	1350	22	−40
	1350	30	−45

* OQ = oil quenched.

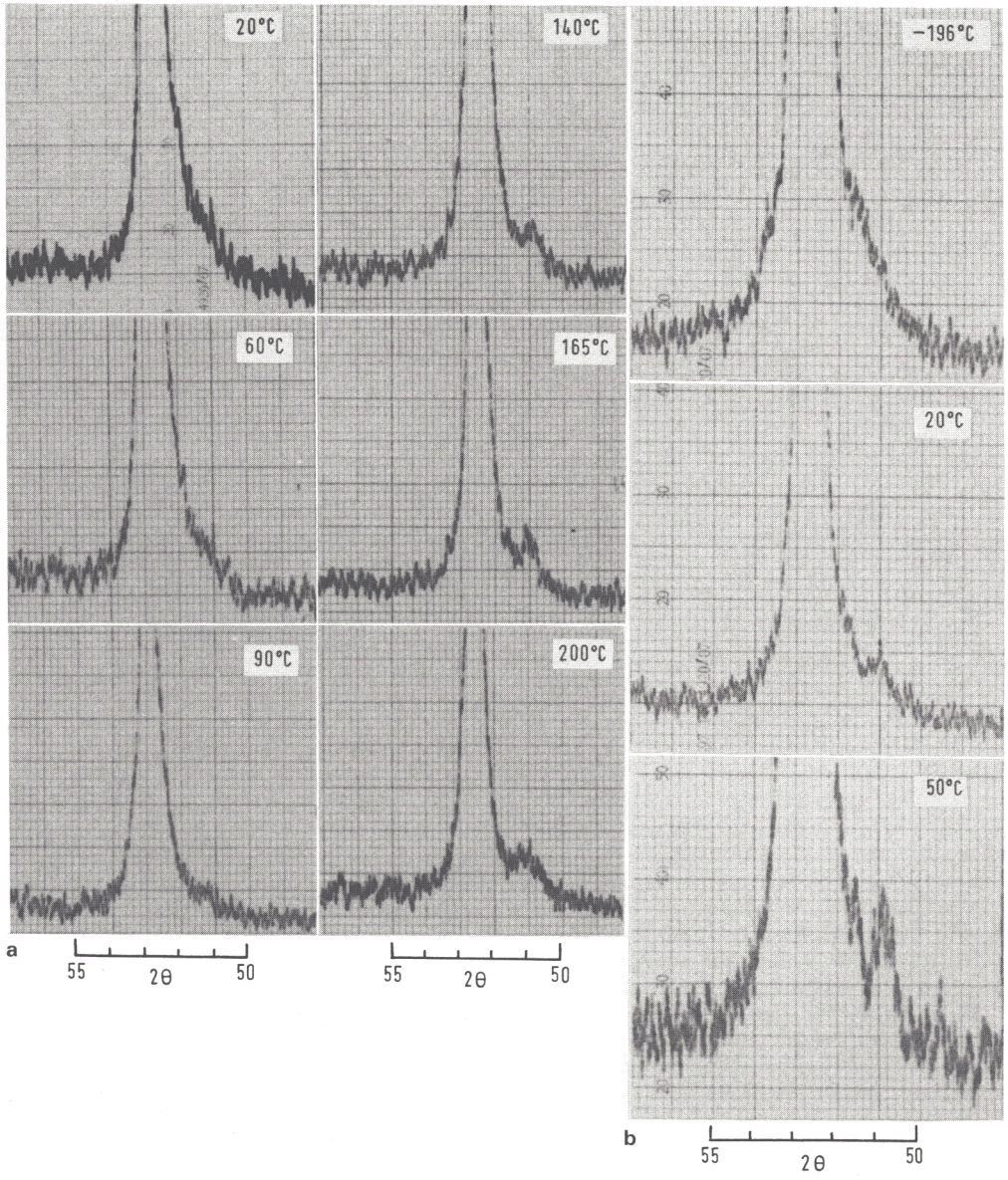

a Fe–0·43C–3·0Mn–2·02Si: heat treatment before impact testing 1080°C for 10 min + isothermal transformation at 295°C for 115 min; *b* Fe–0·39C–4·08Ni–2·05Si: heat treatment before impact testing 880°C for 10 min + isothermal transformation at 340°C for 60 min

7 X-ray analysis (Co K_α radiation) of impact fracture surfaces: specimens had been impact tested at temperatures indicated, and {111} austenite peak occurs at $2\theta \pm 51°$, where θ is corresponding Bragg angle

the easiest to detect. One factor that must be considered is whether it is possible that the presence of any tetragonal martensite introduced by the decomposition of high-carbon retained austenite interferes with the {111} peak. Calculations (based on the x_γ levels given in Table 1 and using Co K_α radiation so that the interference should not be serious) suggested that the tetragonal {110} peak would be expected to appear at least 1·2° distant from the {111} peak.

The diffractometer traces obtained are presented in Fig. 7 as a function of the impact test temperature. The truncated peak is the main {011} bainitic ferrite peak. For both alloys, the {111} peak becomes increasingly significant as the impact test temperature increases. This reflects the expected increasing stability of the austenite as a function of temperature. Clearly, the stability of the austenite (near the crack tip) extends to much lower temperatures for the nickel based steel than for the Fe–0·43C–3·0Mn–2·02Si steel, because the latter contained considerably more blocky austenite (Part 1 and Table 1 above) than the former.

GENERAL CONCLUSIONS

It has been demonstrated in Part 1 that the model based on the mechanism of bainite transformation[2,3] can be successfully applied to the design of strong and tough steels. The properties of the bainitic microstructures studied were

Table 3 Tensile test results

Alloy	Fe–0·22C–3·00Mn–2·03Si	Fe–0·39C–4·08Ni–2·05Si
Ultimate tensile strength, MN m^{-2}	1420	1610
0·2% proof stress, MN m^{-2}	1060	1350
Reduction of area, %	52	56
Elongation (gauge length equal to 5·65 × square root of cross-sectional area)	22	12

certainly superior to the corresponding tempered martensite based microstructures.

Although the present experiments were not intended to provide commercially usable high strength steels, the predicted and tested steels, Fe–0·22C–3·00Mn–2·03Si and Fe–0·39C–4·08Ni–2·05Si, do have excellent properties: it is nevertheless possible that these compositions could be optimized even further.

ACKNOWLEDGMENTS

The authors are grateful to Professor R. W. K. Honeycombe, FRS for the provision of laboratory facilities. Much of this work was financially supported by the Ministry of Defence, Royal Armaments Research and Development Establishment, Fort Halstead and by the Science and Engineering Research Council.

REFERENCES

1. H. K. D. H. BHADESHIA and D. V. EDMONDS: this issue, 411.
2. H. K. D. H. BHADESHIA and D. V. EDMONDS: *Acta Metall.*, 1980, **28**, 1265.
3. H. K. D. H. BHADESHIA: *Acta Metall.*, 1981, **29**, 1117.
4. B. D. CULLITY: in 'Elements of X-ray diffraction', 269; 1967, Reading, Mass., Addison-Wesley.